

# FOCUS: ION-SURFACE COLLISIONS AND PEPTIDE RADICAL CATIONS

---

## Effect of the Surface on Charge Reduction and Desorption Kinetics of Soft Landed Peptide Ions

Omar Hadjar, Peng Wang, Jean H. Futrell, and Julia Laskin

Pacific Northwest National Laboratory, Fundamental Science Directorate, Richland, Washington, USA

Charge reduction and desorption kinetics of ions and neutral molecules produced by soft-landing of mass-selected singly and doubly protonated Gramicidin S (GS) on different surfaces was studied using time dependant *in situ* secondary ion mass spectrometry (SIMS) integrated in a specially designed Fourier transform ion cyclotron resonance mass spectrometer (FT-ICR MS) research instrument. Soft-landing targets utilized in this study included inert self-assembled monolayers (SAMs) of 1-dodecane thiol (HSAM) and its fluorinated analog (FSAM) on gold and hydrophilic carboxyl-terminated (COOH-SAM) and amine-terminated (NH<sub>2</sub>-SAM) surfaces. We observed efficient neutralization of soft-landed ions on the COOH-SAM surface, partial retention of only one proton on the HSAM surface, and efficient retention of two protons on the FSAM surface. Slow desorption rates measured experimentally indicate fairly strong binding between peptide molecules and SAM surfaces with the binding energy of 20–25 kcal/mol. (*J Am Soc Mass Spectrom* 2009, 20, 901–906) Published by Elsevier Inc. on behalf of American Society for Mass Spectrometry

---

Interaction of neutral and charged biomolecules with surfaces is an ubiquitous fundamental phenomenon in biology and one of the most important processes in the development of biomaterials and other biotechnological applications [1, 2]. Because of their complexity our understanding of such interactions is very limited. For example, protein adsorption on substrates is a highly dynamic process that is strongly influenced by Coulomb interactions, hydrogen bonding, and relatively weak noncovalent interactions. These processes are highly dependant on the primary and the higher-order structure of the protein and on the properties of the surface and the solvent.

It has recently been demonstrated that soft-landing (SL) of mass-selected ions on surfaces is a useful mass spectrometric approach for probing details of this intrinsic behavior of immobilized biological molecules that removes the strong effects of solvents [3–5]. SL is defined as intact capture of mass-selected polyatomic ions on substrates [6, 7] and has already been successfully used to study charge retention by small closed-shell ions [6–9] and peptide and protein ions deposited onto self-assembled monolayer surfaces (SAMs) [10–13]. Retention of biological activity (but not charge) by

proteins deposited on liquid [10, 14] and on plasma treated metal surfaces [15] has also been demonstrated.

Recently we reported the first detailed study of the kinetics of desorption and charge reduction following SL of doubly protonated Gramicidin S (GS) onto the FSAM surface [16]. We utilized an in-line 8 keV Cs<sup>+</sup> ion gun that allowed us to interrogate the surface *in situ* and in real time using secondary ion mass spectrometry (SIMS). We followed the evolution of the SIMS spectrum as a function of time during and after the deposition of [GS + 2H]<sup>2+</sup> and obtained unique kinetics signatures for doubly protonated, singly protonated, and neutral peptides retained on the surface. Using the characteristic ion signatures and a kinetic model we measured rate coefficients for charge reduction and thermal desorption of ions and neutral GS molecules from the surface. An important process established in that work was the instantaneous loss of one or two protons by a fraction of ions colliding with the FSAM surface. Collision induced fast charge reduction is followed by very slow proton loss by ions trapped on the surface. Thermal desorption of ionic and neutral species efficiently competes with the charge reduction process.

In this research, we applied the same *in situ* SIMS technique for studying charge-transfer from soft-landed ions to surfaces to establish a molecular level understanding of interactions of different charge states of the model GS peptide with hydrophobic and hydrophilic

---

Address reprint requests to Dr. J. Laskin, Fundamental Sciences Division, Pacific Northwest National Laboratory, P.O. Box 999 K8-88, Richland, WA 99352, USA. E-mail: [Julia.Laskin@pnl.gov](mailto:Julia.Laskin@pnl.gov)

SAMs chosen as appropriate surrogates for different types of biological substrates.

## Experimental

Experiments were performed using a specially designed 6T FT-ICR instrument configured for studying ion–surface interactions [17]. The experimental approach for SL experiments has been described elsewhere [11, 16]. Briefly, mass-selected peptide ions produced in a high-transmission electrospray source undergo normal-incidence collision with a SAM surface positioned at the rear trapping plate of the ICR cell. Ion kinetic energy is controlled by varying the voltage difference between the collisional quadrupole of the ion source and the surface and was maintained at 20 eV/charge in these experiments. During ion SL the surface is exposed to a continuous beam of mass-selected ions and the deposition time is varied between 20 and 150 min. Typical ion currents of 4 and 15 pA of mass-selected singly and doubly protonated ions of gramicidin S, respectively, are delivered onto a ca. 3.5 mm diameter spot on the target. The maximum coverage of soft-landed ions obtained in these experiments does not exceed 12% of a monolayer.

In situ analysis of surfaces following SL is performed by combining 8 keV Cs<sup>+</sup> secondary ion mass spectrometry with FT-ICR detection of the sputtered ions (FT-ICR-SIMS) [16]. Primary Cs<sup>+</sup> ions are generated using a model 101502 HWIG-250F cesium ion gun (HeatWave Labs Inc., Watsonville, CA) that is installed on-axis with the SL target. Static SIMS conditions with a total ion flux of about 10<sup>10</sup> ions/cm<sup>2</sup> (current 4 nA, duration 80  $\mu$ s, spot diameter 4.6 mm, 10 shots per spectrum, ~100 data points) were used in these experiments that typically lasted for 10 to 12 h. The following potentials were applied to various focusing elements: Cs<sup>+</sup> gun floating voltage, +8 kV; extraction, +7 kV; lens, +5 kV; Einzel lens, ( $L_1 = L_2 = -250$  V;  $L_3 = +3$  kV). The Cs<sup>+</sup> ion beam was pulsed by alternating the potential applied to one of the deflection plates between 0 and –400 V the high value being used to block the Cs<sup>+</sup> beam from reaching the surface. Data acquisition was accomplished utilizing a MIDAS data station [18]. Each SIMS spectrum was averaged over 10 shots corresponding to an acquisition time of 10 s. The kinetics data were obtained by sampling the SAM surface every 1.2 min for the first 70 min after the SL and every 10 min for the remainder of the experiment.

SAMs of 1-dodecanethiol (HSAM), 1H, 1H, 2H, 2H-perfluorodecane-1-thiol (FSAM), 11-mercaptopundecanoic acid (COOH-SAM), and 11-amino-1-undecanethiol (NH<sub>2</sub>-SAM) were used as targets for these SL experiments. The surfaces were prepared following literature procedures [19, 20]. Gold coated silicon wafer (5 nm chromium adhesion layer and 100 nm of polycrystalline vapor-deposited gold) was purchased from SPI Supplies (Westchester, PA) and custom laser cut into 4.8 mm diameter substrates by Delaware Diamond Knives

(Wilmington, DE). After thorough cleaning, the substrates were immersed for 12 h in the container with 1 mM solution of the corresponding thiol in ethanol. The SAM surfaces were then removed from the thiol solutions, ultrasonically washed in ethanol (acetic acid/ethanol in the case of COOH-SAM and NH<sub>2</sub>-SAM) for 5 min, quickly dried with dry nitrogen gas, and placed in the UHV chamber.

1H,1H,2H,2H-perfluorodecane-1-thiol was purchased from Fluorous Technologies Inc. (Pittsburgh, PA); 11-amino-1-undecanethiol was purchased from Dojindo Molecular Technologies, (Gaithersburg, MD); 1-dodecanethiol, 11-mercaptopundecanoic acid, and GS were purchased from Sigma-Aldrich (St. Louis, MO). GS was dissolved in a 50:50 (vol/vol) methanol:water solution with 1% acetic acid to a final concentration of 0.1 mg/mL. A syringe pump (Cole Parmer, Vernon Hills, IL) was used for direct infusion of the electrospray samples at a flow rate of 20  $\mu$ L/h.

## Results and Discussion

We previously reported that charge retention and partial neutralization of the doubly protonated GS following soft-landing (SL) onto the FSAM surface results in formation of a mixture of [GS + 2H]<sup>2+</sup>, [GS + H]<sup>+</sup>, and neutral GS molecules on the surface. Each of these species exhibits distinctive charge reduction and desorption kinetics [16]. Energetic bombardment of the surface with the primary Cs<sup>+</sup> beam generates secondary ions characteristic of all three charge states of the peptide. The SIMS spectrum of the FSAM surface obtained following SL of GS contains a small [GS + 2H]<sup>2+</sup> and an abundant [GS + H]<sup>+</sup> peak. In addition, the SIMS spectrum exhibits a number of abundant fragments including LFPV (*m/z* 457.3), PVO (*m/z* 311.2), and PV-28 (*m/z* 169.1) ions readily identified as fragments of neutral GS generated in the desorption/ionization step. Minor SIMS fragment ions, LF and O, follow the kinetics of the doubly protonated species, while no product ions follow the kinetic behavior of the [GS + H]<sup>+</sup> ion. Several fragment ions exhibit mixed behavior suggesting that they originate from different charge states of the peptide formed on the surface as a result of partial retention of the initial charge by a fraction of soft-landed ion along with partial charge reduction and complete neutralization of other deposited doubly protonated precursors.

The present research compared the evolution of the soft-landed peptide ions on inert FSAM and HSAM surfaces and hydrophilic COOH-SAM and NH<sub>2</sub>-SAM surfaces. It should be noted that because SL of mass-selected ions produces highly pure uniform films on substrates it is difficult to compare our results with results obtained using conventional surface preparation methods. We have conducted extensive characterization of peptide films prepared using dried droplet and electrospray deposition approaches [11, 12, 21] and concluded that SIMS spectra obtained for such films are strongly affected

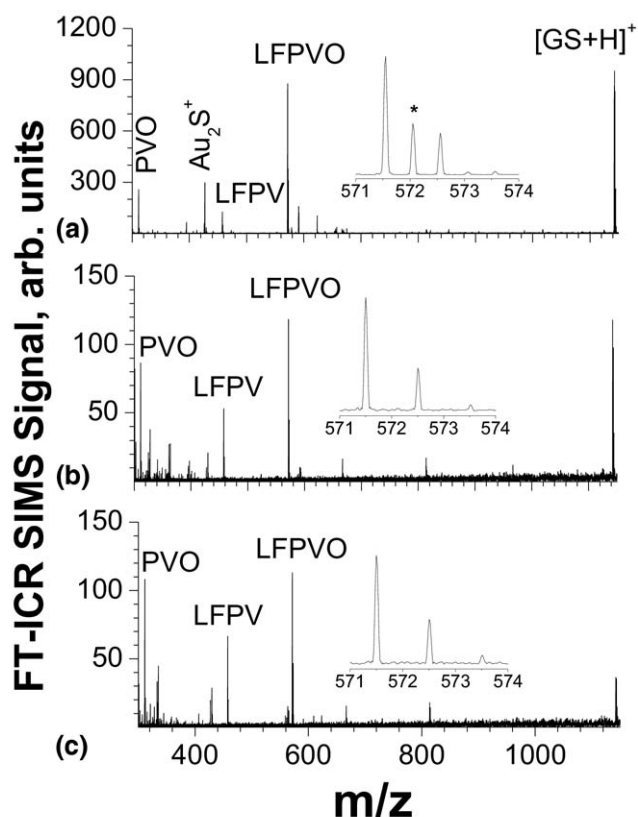


**Figure 1.** FT-ICR SIMS spectra obtained after SL of  $[GS + 2H]^{2+}$  on the (a) FSAM, (b) HSAM, COOH-SAM surfaces.

by the presence of impurities and the morphology of the samples generated during the drying process. SIMS spectra obtained from peptide films prepared using these approaches are more complex than the corresponding spectra obtained from films prepared by SL. Similar peptide-related features are observed in spectra obtained for peptide films prepared on hydrophilic surfaces using both SL and conventional approaches. However, highly non-uniform films are formed on hydrophobic surfaces because the analyte molecules clump together in the drying stage resulting in poor reproducibility of SIMS data.

Figure 1 presents typical 8 keV  $Cs^+$  FT-ICR SIMS spectra obtained after deposition of 20 to 25 pA of mass-selected doubly protonated gramicidin S  $[GS + 2H]^{2+}$  onto a 3 mm spot on the FSAM, HSAM, and COOH-SAM surfaces. The deposition time was adjusted between 24 and 28 min to ensure similar surface coverage of ca. 4% of a monolayer in these experiments. Surface coverage was estimated from the known ion exposure using the spot size of 3.5 mm in diameter and 263 Å cross section of  $[GS + 2H]^{2+}$  [12, 16]. All three spectra are dominated by the peak at  $m/z$  571.4. Our previous study demonstrated that this peak is composed of the symmetric LFPVO fragment of GS and the doubly protonated  $[GS + 2H]^{2+}$  ion [16]. The latter is accompanied by the  $^{13}C$  isotopic peak at  $m/z$  571.9. The inserts in Figure 1 demonstrate that the  $^{13}C$  isotopic

peak of the  $[GS + 2H]^{2+}$  ion is observed only on the FSAM surface suggesting that the 571.4 peak observed in SIMS spectra of the HSAM and COOH-SAM surfaces corresponds to the LFPVO fragment ion with no contribution of the doubly protonated GS species. It follows that HSAM and COOH-SAM surfaces do not retain any doubly protonated peptides deposited in our experiments.

It is noteworthy that no peptide-related peaks were observed in the SIMS spectrum when the  $NH_2$ -SAM surface was used as a target. It is also noted that only a very weak SIMS signal was obtained for this surface before ion deposition. One possible explanation for these observations is that poor organization of the SAM and more efficient charge-transfer in the SIMS plume because of the presence of basic nitrogen-containing species could significantly suppress the peptide signal on this surface. Alternatively, the low peptide signal may be attributed to the decrease in the SL efficiency; this decreased efficiency may result from partial protonation of terminal amino groups and accumulation of the net positive charge on the  $NH_2$ -SAM surface. Future studies will address this intriguing result in more detail.

Another notable difference between SIMS spectra obtained for the three different surfaces is the relative abundance of the  $[GS + H]^+$  ion. It decreases in the order FSAM  $\geq$  HSAM  $>$  COOH-SAM. This observation is consistent with the results reported for SL of the singly protonated angiotensin III on the FSAM, HSAM, and COOH-SAM surfaces [12]. In that study the low sputtered signal obtained following SL on COOH-SAM was attributed to more efficient neutralization of ions on the surface relative to FSAM and HSAM surfaces. The decrease in the  $[GS + H]^+$  signal is accompanied by an increase in the signal of the PVO internal fragment at  $m/z$  311.2. Since this fragment is generated from neutral GS desorbed in SIMS experiments while most of the  $[GS + H]^+$  signal comes from singly protonated species retained on the surface the  $[GS + H]^+/PVO$  ratio is a measure of the relative abundance of protonated and neutral GS trapped on the surface. This ratio decreases in the order FSAM  $>$  HSAM  $>$  COOH-SAM, indicating much higher neutralization efficiency following SL on the hydrophilic COOH-SAM surface relative to inert HSAM and FSAM surfaces.

Figure 2 shows the time dependence of the abundance of  $[GS + H]^+$  and PVO ions representing the singly protonated and neutral species on the surface normalized to the abundance of the surface peak  $Au_2SH^+$  at  $m/z$  426.9. These kinetics plots were recorded immediately following the ion deposition step. Clearly these two ions exhibit different kinetic signatures on different surfaces. The results obtained for the FSAM surface are consistent with our previous study [16]. Specifically, the  $[GS + 2H]^{2+}$  ion exhibits relatively rapid decay (data not shown, see Figure 3b of reference [16]), while the  $[GS + H]^+$  ion continues to increase for 2 to 3 h after ion deposition is concluded. Kinetic modeling demonstrated that this behavior reflects rela-

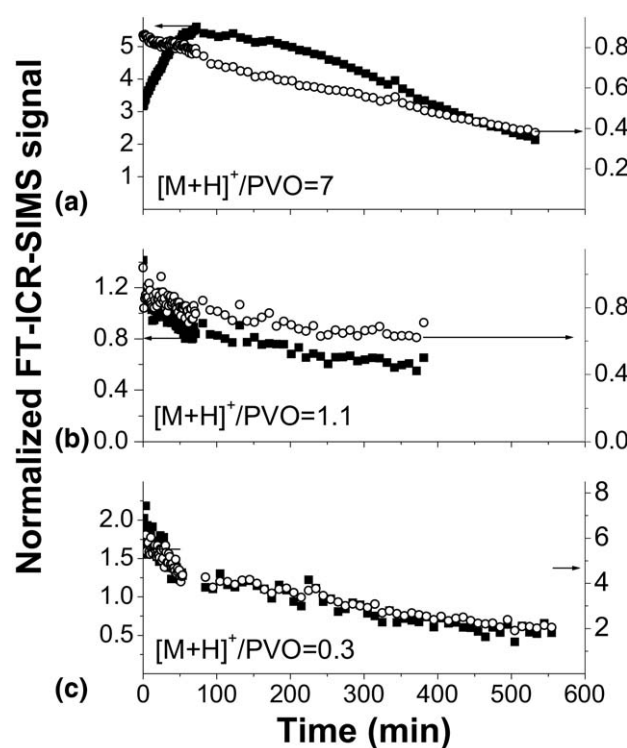


**Figure 2.** Kinetic plots for  $[GS + H]^+$  ( $m/z$  1142, filled squares) and PVO ( $m/z$  311, open circles) ions obtained after SL of  $[GS + 2H]^{2+}$  on the (a) FSAM, (b) HSAM, COOH-SAM surfaces. Note that the normalized abundances of  $[GS + H]^+$  and PVO are shown on the left and right axes, respectively. Signal intensities were normalized to the abundance of the  $Au_2S^+$  ion ( $m/z$  427) for the FSAM surface, and the  $C_3H_5S^+$  peak ( $m/z$  73) for the HSAM and COOH-SAM surface. The average  $[GS + H]^+/PVO$  ratio is labeled on each plot.

tively slow proton loss from the soft-landed doubly protonated GS to generate  $[GS + H]^+$  ions on the surface. It is interesting to note that the  $[GS + Au]^+$  peak observed in the SIMS spectrum for the FSAM surface (not shown) follows similar kinetics as the  $[GS + H]^+$  peak. Evidently, this ion is formed by gas-phase cation exchange from the singly protonated GS desorbed during SIMS analysis. In contrast, the neutral species on all three surfaces for which the PVO fragment ion is diagnostic follows an almost linear decrease after ion deposition. Similar, almost linear, decay is observed for the  $[GS + H]^+$  ion on the HSAM and COOH-SAM surfaces. This is further confirmation that the  $[GS + 2H]^{2+}$  ion is not retained on these surfaces. However, the  $[GS + H]^+$  ion follows somewhat faster decay on HSAM than on the COOH-SAM surface.

The average  $[GS + H]^+/PVO$  ratio shown in Figures 2 and 3 decreases in the order FSAM > HSAM > COOH-SAM for both charge states of soft-landed GS. While the PVO fragment uniquely characterizes neutral peptide molecules on the surface, the  $[GS + H]^+$  ion is formed by both ionization of neutral molecules during SIMS analysis and by desorption of singly protonated species retained on the surface. Identical kinetic behavior obtained for the PVO and the  $[GS + H]^+$  ion on the

COOH-SAM surface implies that soft-landed GS ions are completely neutralized on this target. Re-ionization of deposited neutral molecules results in extensive fragmentation and a relatively low  $[GS + H]^+/PVO$  ratio of 0.1–0.3. For the HSAM surface the substantially higher  $[GS + H]^+/PVO$  ratio of 1.1–2 indicates that this surface retains some singly protonated GS molecules. The highest  $[GS + H]^+/PVO$  ratio of 7–11 obtained for FSAM indicates that this surface has the highest efficiency for charge retention.

Decay rates for the neutral and singly protonated species on the HSAM and COOH-SAM surfaces obtained from the first-order kinetic fitting of the experimental data are summarized in Table 1. Rate constants for the decay of  $[GS + H]^+$  and PVO ions on the FSAM surface were obtained from the detailed kinetic modeling described in our previous paper [16]. Briefly, our model for charge reduction by soft-landed species on the surface includes as contributing processes the loss of a proton, thermal desorption of ions and neutral GS molecules from the surface, re-ionization of both neutral and singly-protonated molecules in SIMS and fast proton loss by soft-landed ions during ion-surface collision.

Figure 4 compares the experimental data and modeling results for  $[GS + H]^+$  ion intensity observed during and after the deposition of singly and doubly protonated GS onto the FSAM surface. Our results for  $[GS + H]^+$  projectile deposited onto the FSAM surface show that the singly protonated GS retained on the

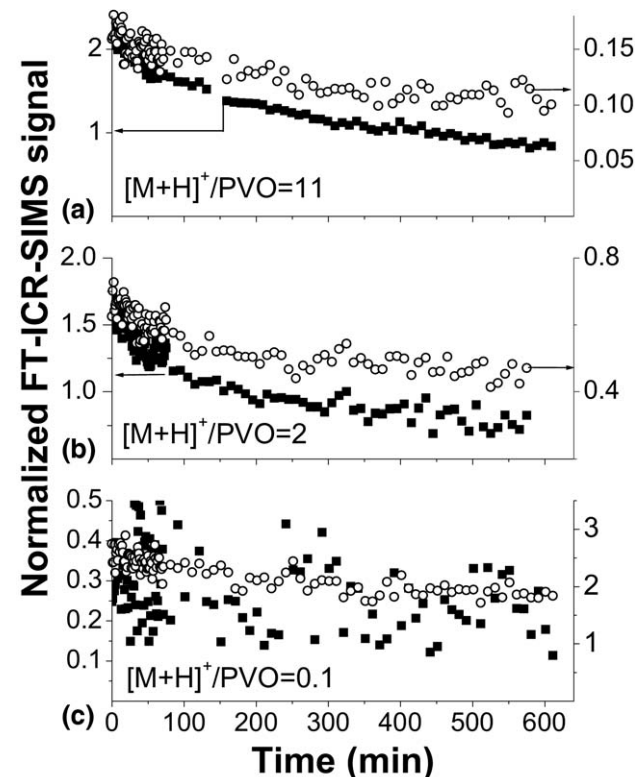


**Figure 3.** Same as Figure 2 for the  $[GS + H]^+$  projectile ion.

**Table 1.** Decay rates in  $\text{min}^{-1}$  obtained from the first-order kinetic fitting of the experimental data

Projectile ion	$[\text{GS} + 2\text{H}]^{2+}$		$[\text{GS} + \text{H}]^+$		
	Surface	$[\text{M} + \text{H}]^+$	PVO	$[\text{M} + \text{H}]^+$	PVO
FSAM		$6 \times 10^{-4}*_{\text{}}$	$1 \times 10^{-3}*$	$2.1 \times 10^{-3}^{\dagger}_{\text{}}$	$1.2 \times 10^{-3}^{\dagger}_{\text{}}$
HSAM		$1.6 \times 10^{-3}$	$9 \times 10^{-4}$	$1.7 \times 10^{-3}$	$9 \times 10^{-4}$
COOH-SAM		$2.3 \times 10^{-3}$	$1.9 \times 10^{-3}$	$1.2 \times 10^{-3}$	$8 \times 10^{-4}$

\*Adopted from reference [16].

<sup>†</sup>Obtained from the detailed kinetic modeling of the data shown in Figure 4.

surface decays mainly by thermal desorption. The rate of proton loss is at least two orders of magnitude slower than the rate of desorption. This result is in excellent agreement with our previous study that examined the evolution of surface-retained  $[\text{GS} + \text{H}]^+$  ion following deposition of the corresponding doubly protonated precursor,  $[\text{GS} + 2\text{H}]^{2+}$  [16]. Because proton loss by the  $[\text{GS} + \text{H}]^+$  ion is an extremely slow process, the evolution of soft-landed species on all three surfaces is dominated by slow desorption of both neutral and singly protonated GS following remarkably similar kinetics. The notable exception is the kinetics for the  $[\text{GS} + \text{H}]^+$  ion following SL of  $[\text{GS} + 2\text{H}]^{2+}$  on the FSAM surface; here the dominant mechanism is proton loss from the retained  $[\text{GS} + 2\text{H}]^{2+}$  ion.

The results obtained in this study are qualitatively consistent with the results of ex situ analysis of the FSAM, HSAM, and COOH-SAM surfaces following SL of peptide ions reported previously [13]. In our ex situ study surfaces were exposed to laboratory air before off-line analysis using standard time-of-flight secondary ion mass spectrometry (TOF-SIMS). We concluded that doubly protonated peptides are readily neutralized by exposure to laboratory air but some singly proton-

ated species are retained on both FSAM and HSAM surfaces. Substantially higher abundance of fragment ions observed for the COOH-SAM surface was attributed to essentially complete neutralization of soft-landed species. However, in this ex situ experiment we could not establish whether ions were neutralized during deposition or after exposure to the ambient environment. The present ultrahigh vacuum in situ investigation clearly demonstrates the occurrence of very fast neutralization of doubly protonated GS on the HSAM surface and fast complete neutralization on the COOH-SAM surface.

## Conclusions

In this work we utilized time-resolved in situ FT-ICR SIMS for quantitative characterization of the effect of the surface on charge retention and desorption following SL of singly and doubly protonated GS on SAM surfaces. Our results demonstrate that the desorption kinetics of ions and neutral peptide molecules retained on different surfaces is characterized by similar rates. In contrast, charge retention by soft-landed ions strongly depends on the properties of the surface. Specifically, while the FSAM surface efficiently retains both doubly and singly protonated peptide molecules, only a small amount of singly charged ions is retained on the HSAM surface and complete neutralization is observed on the COOH-SAM. Very efficient charge retention on the FSAM surface determines characteristically different kinetic behavior for  $[\text{GS} + \text{H}]^+$  ion following deposition of the singly and doubly protonated GS on these substrates. In contrast, kinetic plots obtained for both HSAM and COOH-SAM surfaces are relatively independent of the initial charge state of the precursor ion.

Assuming pre-exponential factors in the range of  $10^{10}\text{--}10^{13} \text{ s}^{-1}$  the measured desorption rates lead to an estimated binding energy of 20–25 kcal/mol between the deposited peptides and the different surfaces investigated here. This binding energy is consistent with the previously reported value derived from desorption kinetics of Substance P from the FSAM surface [12]. Finally, instantaneous proton loss is the major neutralization pathway for soft-landed protonated peptides. In future work we shall explore the unexpectedly low SL efficiency noted for amine-terminated SAMs.

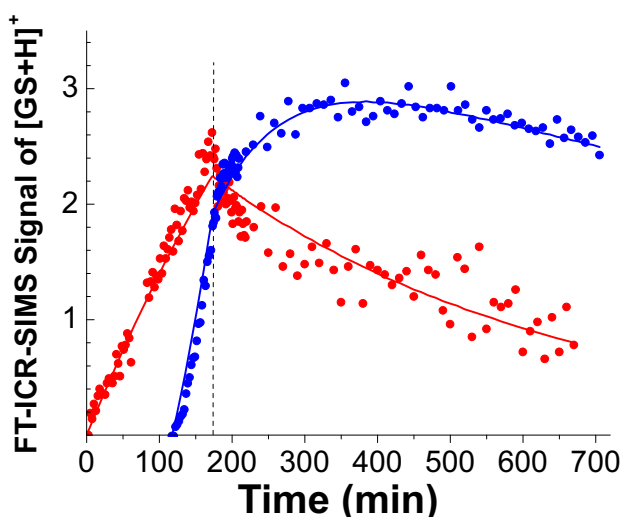


**Figure 4.** Kinetic plots obtained for the  $[\text{GS} + \text{H}]^+$  ion following deposition of  $[\text{GS} + 2\text{H}]^{2+}$  (blue) and  $[\text{GS} + \text{H}]^+$  (red). The curves are aligned along the x-axis at the time marked with the dashed line that corresponds to the end of SL. The results of the kinetic modeling are shown as solid lines.

## Acknowledgments

The authors acknowledge support for this work by a grant from the Chemical Sciences Division, Office of Basic Energy Sciences of the U.S. Department of Energy (DOE), and the Laboratory Directed Research and Development Program at the Pacific Northwest National Laboratory (PNNL). The work was performed at the W. R. Wiley Environmental Molecular Sciences Laboratory (EMSL), a national scientific user facility sponsored by the U.S. DOE of Biological and Environmental Research and located at PNNL. PNNL is operated by Battelle for the U.S. DOE.

## References

- Gray, J. J. The interaction of proteins with solid surfaces. *Curr. Opin. Struct. Biol.* 2004, 14, 110–115.
- Latour, R. A. Biomaterials: Protein-Surface Interactions. In *Encyclopedia of Biomaterials and Biomedical Engineering*; Wnek, G.; Bowlin, G., Eds.; Taylor and Francis: New York, 2005.
- Gologan, B.; Wiseman, J. M.; Cooks, R. G. Ion Soft Landing: Instrumentation, Phenomena, and Applications. In *Principles of Mass Spectrometry Applied to Biomolecules*; Laskin, J.; Lifshitz, C., Eds.; John Wiley and Sons: Hoboken, NJ, 2006.
- Laskin, J.; Wang, P.; Hadjar, O. Soft-landing of peptide ions onto self-assembled monolayer surfaces: an overview. *Phys. Chem. Chem. Phys.* 2008, 10, 1079–1090.
- Volny, M.; Sengupta, A.; Wilson, C. B.; Swanson, B. D.; Davis, E. J.; Turecek, F. Surface-enhanced Raman spectroscopy of soft-landed polyatomic ions and molecules. *Anal. Chem.* 2007, 79, 4543–4551.
- Miller, S. A.; Luo, H.; Pachuta, S. J.; Cooks, R. G. Soft-landing of polyatomic ions at fluorinated self-assembled monolayer surfaces. *Science* 1997, 275, 1447–1450.
- Gologan, B.; Green, J. R.; Alvarez, J.; Laskin, J.; Cooks, R. G. Ion/surface reactions and ion soft-landing. *Phys. Chem. Chem. Phys.* 2005, 7, 1490–1500.
- Luo, H.; Miller, S. A.; Cooks, R. G.; Pachuta, S. J. Soft landing of polyatomic ions for selective modification of fluorinated self-assembled monolayer surfaces. *Int. J. Mass Spectrom.* 1998, 174, 193–217.
- Volny, M.; Elam, W. T.; Ratner, B. D.; Turecek, F. Preparative soft and reactive landing of gas-phase ions on plasma-treated metal surfaces. *Anal. Chem.* 2005, 77, 4846–4853.
- Gologan, B.; Takats, Z.; Alvarez, J.; Wiseman, J. M.; Talaty, N.; Ouyang, Z.; Cooks, R. G. Ion soft-landing into liquids: Protein identification, separation, and purification with retention of biological activity. *J. Am. Soc. Mass Spectrom.* 2004, 15, 1874–1884.
- Alvarez, J.; Cooks, R. G.; Barlow, S. E.; Gaspar, D. J.; Futrell, J. H.; Laskin, J. Preparation and in situ characterization of surfaces using soft landing in a Fourier transform ion cyclotron resonance mass spectrometer. *Anal. Chem.* 2005, 77, 3452–3460.
- Alvarez, J.; Futrell, J. H.; Laskin, J. Soft-landing of peptides onto self-assembled monolayer surfaces. *J. Phys. Chem. A* 2006, 110, 1678–1687.
- Laskin, J.; Wang, P.; Hadjar, O.; Futrell, J. H.; Alvarez, J.; Cooks, R. G. Charge retention by peptide ions soft-landed onto self-assembled monolayer surfaces. *Int. J. Mass Spectrom.* 2007, 265, 237–243.
- Ouyang, Z.; Takats, Z.; Blake, T. A.; Gologan, B.; Guymon, A. J.; Wiseman, J. M.; Oliver, J. C.; Davission, V. J.; Cooks, R. G. Preparing protein microarrays by soft-landing of mass-selected ions. *Science* 2003, 301, 1351–1354.
- Volny, M.; Elam, W. T.; Branca, A.; Ratner, B. D.; Turecek, F. Preparative soft and reactive landing of multiply charged protein ions on a plasma-treated metal surface. *Anal. Chem.* 2005, 77, 4890–4896.
- Hadjar, O.; Futrell, J. H.; Laskin, J. First observation of charge reduction and desorption kinetics of multiply protonated peptides soft landed onto self-assembled monolayer surfaces. *J. Phys. Chem. C* 2007, 111, 18220–18225.
- Laskin, J.; Denisov, E. V.; Shukla, A. K.; Barlow, S. E.; Futrell, J. H. Surface-induced dissociation in a Fourier transform ion cyclotron resonance mass spectrometer: Instrument design and evaluation. *Anal. Chem.* 2002, 74, 3255–3261.
- Senko, M. W.; Canterbury, J. D.; Guan, S. H.; Marshall, A. G. A high-performance modular data system for Fourier transform ion cyclotron resonance mass spectrometry. *Rapid Commun. Mass Spectrom.* 1996, 10, 1839–1844.
- Chidsey, C. E. D.; Liu, G. Y.; Rountree, P.; Scoles, G. Molecular order at the surface of an organic monolayer studied by low-energy helium diffraction. *J. Chem. Phys.* 1989, 91, 4421–4423.
- Wang, H.; Chen, S. F.; Li, L. Y.; Jiang, S. Y. Improved method for the preparation of carboxylic acid and amine terminated self-assembled monolayers of alkanethiolates. *Langmuir* 2005, 21, 2633–2636.
- Hadjar, O.; Wang, P.; Futrell, J. H.; Dessiaterik, Y.; Zhu, Z.; Cowin, J. P.; Iedema, M. J.; Laskin, J. Design and Performance of a New Instrument for Soft-Landing of Biomolecular Ions on Surfaces. *Anal. Chem.* 2007, 79, 6567–6574.